
Statistical Distance Based Deterministic Offspring Selection in SMC Methods

Oskar Kviman^{1,2} Hazal Koptagel^{1,2} Harald Melin^{1,2} Jens Lagergren^{1,2}

Abstract

Over the years, sequential Monte Carlo (SMC) and, equivalently, particle filter (PF) theory has gained substantial attention from researchers. However, the performance of the resampling methodology, also known as offspring selection, has not advanced recently. We propose two deterministic offspring selection methods, which strive to minimize the Kullback-Leibler (KL) divergence and the total variation (TV) distance, respectively, between the particle distribution prior and subsequent to the offspring selection. By reducing the statistical distance between the selected offspring and the joint distribution, we obtain a heuristic search procedure that performs superior to a maximum likelihood search in precisely those contexts where the latter performs better than an SMC. For SMC and particle Markov chain Monte Carlo (pMCMC), our proposed offspring selection methods always outperform or compare favorably with the two state-of-the-art resampling schemes on two models commonly used as benchmarks from the literature.

1. Introduction

Since the bootstrap particle filter (BPF) and multinomial resampling were both proposed in the seminal work of Gordon et al. (1993), sequential Monte Carlo (SMC) methods have been heavily researched and applied to a variety of problems, such as robotics (Grisetti et al., 2005; Eade & Drummond, 2006), phylogenetic tree inference (Bouchard-Côté et al., 2012), econometrics (Pitt & Shephard, 1999), and much more. There are two important explanations for its popularity. First, given a Bayesian model of any complex, non-linear or/and non-Gaussian dynamical system, SMC algorithms, interchangeably referred to as particle filters (PFs), produce impressive solutions without simplification

of the model. Second, it is straightforward to understand, at least informally, how the PF works.

Following the invention of the BPF, advanced improvements have been proposed. The BPF is likely the simplest possible PF as it employs the model prior as its proposal distribution, and so, in attempts to obtain more sophisticated PFs, designing clever proposals has gained attention. For instance, the auxiliary PF (Pitt & Shephard, 1999) utilizes future observations in order to improve the proposals. Not long ago, Naesseth et al. (2017) presented a proposal distribution with parameters which were tuned using variational inference (VI). Another example of combining VI and SMC is given in Maddison et al. (2017), where they derive an alternative to the evidence lower bound (ELBO) by letting a variant of the PF's log-likelihood be an objective function, which can be used for gradient descent minimization. Also, Saeedi et al. (2017) attempt to simultaneously update a complete set of trajectories from an earlier PF run by maximizing the ELBO objective. But as their method takes a posterior approximation as input, it is more appropriately compared with, e.g., a particle Markov chain Monte Carlo (pMCMC) method. Although they do not utilize VI, both Fox (2002) and Soto (2005) use the Kullback-Leibler (KL) divergence between the target distribution (making simplifying assumptions on the form of the target distribution) and the approximation to adapt the number of particles in the PF.

However, it appears that since VI's rise in popularity in the late 90's (Jordan et al., 1999), little attention has been devoted to SMC's offspring selection – often referred to as the resampling step, as it is typically done stochastically. Common resampling schemes, all stochastic, are; stratified and systematic resampling (Kitagawa, 1996), multinomial resampling (Gordon et al., 1993) and residual resampling (Higuchi, 1997; Liu & Chen, 1998). In this work, we will use the stratified and systematic resampling schemes as baselines, since they are seemingly the most popular (Douc & Cappé, 2005; Doucet et al., 2001; Andrieu et al., 2010). Deterministic resampling schemes exist, albeit they do often not compare with the standard stochastic ones (mentioned above) in terms of estimation capabilities (Kitagawa, 1996), or they are not off-the-shelf methods and are difficult to fit into the established theoretical framework surrounding SMC methods (Li et al., 2012).

¹Department of Electrical Engineering and Computer Science, KTH Royal Institute of Technology, Stockholm, Sweden ²Science for Life Laboratory, Stockholm, Sweden.

Correspondence to: Oskar Kviman <okviman@kth.se>, Jens Lagergren <jens.lagergren@scilifelab.se>.

In this work, we present a set of novel methods¹ for performing offspring selection in PFs, based on minimization of statistical distances. Specifically, we design (1) a reshuffling algorithm that given a normalized particle distribution finds an unweighted particle distribution with minimum KL divergence and (2) another reshuffling algorithm that given the same input finds an unweighted particle distribution with minimal total variation (TV) distance. We prove in the Supplementary Materials that each of these two reshuffling algorithms attains unweighted particle distributions on minimal statistical distance. Our reshuffling schemes are off-the-shelf methods, ready to be used in place of standard resampling techniques – without manipulation of the SMC algorithm.

2. Notation and Background Information

In this section, we introduce the BPF and the state-of-the-art offspring selection schemes.

2.1. The Bootstrap Particle Filter

The PF approximates the intractable posterior distribution, $p(x_{1:n}|y_{1:n})$, via a particle distribution (Doucet & Johansen, 2009; Doucet et al., 2001)

$$q(x_{1:n}) = \sum_s w_n^s \delta^s(x_{1:n}), \quad (1)$$

where δ^s denotes a Dirac distribution at point $s \in S$, and w_n^s is the s 'th particle's normalized importance weight at time $n \in N$. The unnormalized weight is

$$\tilde{w}_n = \frac{p(x_{1:n}, y_{1:n})}{\pi(x_{1:n})} = \frac{g(y_n|x_n)f(x_n|x_{n-1})}{\pi(x_n|x_{1:n-1})} \tilde{w}_{n-1}^{1-\mathbb{1}_{R_n}}, \quad (2)$$

where $g(y_n|x_n)$ and $f(x_n|x_{n-1})$ are the model's emission and transition probabilities, respectively, $\mathbb{1}_{R_n}$ is the indicator function, and R_n is the event that resampling occurred at time n^2 .

Throughout this work, we will only consider the transition distribution as our proposal distribution, i.e. $\pi(x_n|x_{n-1}) = f(x_n|x_{n-1})$. Doing so, we end up with BPF, the simplest possible PF, and Equation 2 now becomes

$$\tilde{w}_n = g(y_n|x_n) \tilde{w}_{n-1}^{1-\mathbb{1}_{R_n}}. \quad (3)$$

Although more advanced PFs exists, the BPF's simplicity makes it useful for demonstrating novel techniques – i.e.

¹Code available at github.com/Lagergren-Lab/KL-TV-Reshuffling

²Setting the \tilde{w}_{n-1} to 1 or $1/S$ will not matter as \tilde{w}_n is later normalized.

Algorithm 1 The Bootstrap Particle Filter

Input: $S, \{y_n\}_{n=1}^N$
Output: $q(x_{1:N})$
 initialize $x_1^s \sim \mu(x_1)$
 compute $\tilde{w}_1^s = g(y_1|x_1^s)$
 normalize $w_1^s = \tilde{w}_1^s / (\sum_s \tilde{w}_1^s)$
for $n = 2, \dots, N$ **do**
 if $\sum_s (w_{n-1}^s)^{-2} < S/2$ **then**
 select ancestors $\{i_n^s\}_{s=1}^S = \mathcal{R}(\{w_{n-1}^s\}_{s=1}^S)$
 set $\tilde{w}_{n-1}^s = 1, \forall s$
 else
 set $i_n^s = s, \forall s$
 end if
 propagate $x_n^s \sim f(x_n^s|x_{n-1}^{i_n^s})$
 compute $\tilde{w}_n^s = g(y_n|x_n^s) \tilde{w}_{n-1}^{i_n^s}$
 normalize $w_n^s = \tilde{w}_n^s / (\sum_s \tilde{w}_n^s)$
end for
return $q(x_{1:N})$

if a new resampling/reshuffling scheme can boost the performance of the BPF, it is reasonable that more advanced methods should benefit it too.

An algorithmic description of the BPF is given in Algorithm 1. Note that i_n^s denotes the ancestor index of particle $x_{1:n}^s$, and that \mathcal{R} is an arbitrary *resampling* or *reshuffling* scheme, i.e., an offspring selection method.

2.2. The Bootstrap Particle Filter with Likelihood

A subset of our proposed reshuffling methods works with the particle likelihoods, $p(x_{1:n}, y_{1:n})$. These methods require some updates to the standard BPF algorithm shown in Algorithm 1. To this end, we provide an updated BPF algorithm, *BPF with likelihood*. The algorithm is available in the Supplementary Materials.

2.3. Offspring Selection

Offspring selection is useful for discarding particles with low importance weights and replacing them with more promising ones. Once a particle $x_{1:n}$ is discarded, a surviving particle is multiplied. This ‘‘circle of life’’-like heuristic ensures that there are constantly S particles in the system. Specifically, offspring selection attempts to replace the particle distribution in Equation 1, by a distribution in terms of particle multiplicities,

$$\check{q}(x_{1:n}) = \frac{1}{S} \sum_s a_n^s \delta^s(x_{1:n}), \quad (4)$$

where $a_n^s \in \mathbb{Z}_0^+$ is the multiplicity of particle s at time n . In other words, a traditional resampling scheme attempts to

approximate $q(x_{1:n})$ using the set of multiplicities

$$\mathcal{A}^S = \{a \in (\mathbb{Z}_0^+)^S : \sum_s a^s = S\}. \quad (5)$$

The notion of approximating $q(x_{1:n})$, which in turn approximates the target posterior distribution $p(x_{1:n}|y_{1:n})$ might seem confusing, but in order to perform offspring selection, we require a mapping from importance weights to particle multiplicities, $(\mathbb{R}_0^+)^S \mapsto \mathcal{A}^S$.

After resampling, the S offspring are regarded as equiprobable, yielding

$$\check{q}(x_{1:n}) = \frac{1}{S} \sum_s \delta^s(x_{1:n}). \quad (6)$$

Obviously, q from Equation 1 is the closest to the target distribution as \check{q} and \tilde{q} are mere approximations of q .

In this work, we compare our proposed methods with the state-of-the-art *stratified* and *systematic* resampling schemes.

The stratified resampling method is inspired by ideas within survey sampling (Douc & Cappé, 2005), i.e. samples should also represent areas with less (probability) density, in an attempt to avoid all particles being centered around modes. To perform stratified resampling, one generates S random numbers according to $u_k = ((k-1) + \tilde{u}_k)/S$, $\tilde{u}_k \sim \mathcal{U}\{0, 1\}$.

These numbers are then used to sample the new index, $s' \in [1, S]$ for each particle, such that $u_{s'} \in [\sum_{s=1}^{s'-1} w_n^s, \sum_{s=1}^{s'} w_n^s)$.

Systematic resampling is similar to the stratified counterpart, only here a single random number is drawn $\tilde{u}_1 \sim \mathcal{U}\{0, \frac{1}{S}\}$ followed by deterministic assignments of the remaining $S-1$ values, $u_k = \tilde{u}_1 + (k-1)/S$.

Finally, in order to have a baseline for our likelihood based methods, we introduce a simple maximum likelihood resampling approach, which we will refer to as **ML**. In ML, only the particle s with the highest likelihood, $p(x_{1:n}^s, y_{1:n})$, is multiplied.

3. Kullback-Leibler Reshuffling

The KL divergence between two distributions q and r , defined as

$$\text{KL}(q(x)||r(x)) = \mathbb{E}_q \left[\log \frac{q(x)}{r(x)} \right], \quad (7)$$

measures the similarity of two distributions, is non-negative and only zero when the distributions are identical.

Algorithm 2 Kullback-Leibler Reshuffling

Input: $\{u^s\}_{s=1}^S$
Output: $\{i^s\}_{s=1}^S$
 order $u^1 \geq \dots \geq u^S$
 set $a^s = 0, \forall s$
 define $C^+(a, s) = f(a+1, s) - f(a, s)$
while $\sum_s a^s < S$ **do**
 compute $t = \text{argmax}_s C^+(a_s, s)$
 set $a^t = a^t + 1$
end while
 map $\{i^s\}_{s=1}^S = h(\{a^s\}_{s=1}^S)$
return $\{i^s\}_{s=1}^S$

3.1. Weight Based KL Reshuffling

Recall from Section 2.3 that $\check{q}(x_{1:n})$ is an approximation of the $q(x_{1:n})$. The goal of weight based KL reshuffling, KL_w is to minimize the KL divergence from $\check{q}(x_{1:n})$ to $q(x_{1:n})$, or equivalently maximize the negative KL divergence. Equation 8 shows the function to be maximized.

$$\begin{aligned} \mathcal{L}(x_{1:n}) &= -\text{KL}(\check{q}(x_{1:n})||q(x_{1:n})) \\ &= \sum_s \check{q}(x_{1:n}^s) \log \frac{q(x_{1:n}^s)}{\check{q}(x_{1:n}^s)} \\ &\propto \sum_s a^s \log \frac{w^s}{a^s}, \end{aligned} \quad (8)$$

where a^s is the multiplicity of the s th particle.

Algorithm 2 is our novel algorithm for finding the optimal unweighted particle distribution \check{q}^* w.r.t. KL divergence. For brevity we let $f(a, s) = a^s \log \frac{w^s}{a^s}$. When the inputs are the importance weights of the particles, $u^s = w^s, \forall s$, the method is referred to as KL_w . The proof showing that we indeed find \check{q}^* is given in the Supplementary Materials.

In short, the algorithm greedily multiplies the particle with index t that contributes the most to maximizing $\mathcal{L}(x_{1:n})$. C^+ function measures how much is gained *and* lost by incrementing the multiplicity of a particle. We introduced a mapping function, h , which partitions the multiplicities of the particles, $\{a^s\}_{s=1}^S$ to particle indices in a natural way.

The KL reshuffling can be implemented using heap data structures so that it runs in $O(S \log S)$ time.

3.2. Likelihood Based KL Reshuffling

In addition to the importance weight based approach, we propose a reshuffling method based on the particle likelihoods, KL_p . This will turn out to provide an excellent alternative to an ML based search heuristic.

Here, we focus on the KL divergence between the par-

ticle distribution and the posterior distribution ($r(x) = p(x_{1:n}|y_{1:n})$). Minimizing the expression in Equation 7 involves handling the intractable distribution, so we approach it from another angle. Since the marginal log-likelihood is fixed and the KL divergence is non-negative, we may instead maximize the ELBO (Jordan et al., 1999), i.e.,

$$\begin{aligned} \mathcal{L}(x_{1:n}) &= \log p(y_{1:n}) - \text{KL}(q(x_{1:n})||p(x_{1:n}|y_{1:n})) \\ &= \mathbb{E}_q \left[\log \frac{p(x_{1:n}, y_{1:n})}{q(x_{1:n})} \right]. \end{aligned} \quad (9)$$

Consequently, minimizing the KL divergence is equivalent to maximizing the ELBO. By plugging in the particle distribution from Equation 1 and later Equation 4 into the ELBO in Equation 9, we obtain

$$\begin{aligned} \mathcal{L}(x_{1:n}) &= \sum_{s=1}^S q(x_{1:n}^s) \log \frac{p(x_{1:n}^s, y_{1:n})}{q(x_{1:n}^s)} \\ &= \sum_{s=1}^S \tilde{q}(x_{1:n}^s) \log \frac{p(x_{1:n}^s, y_{1:n})}{\tilde{q}(x_{1:n}^s)} \\ &= \sum_{s=1}^S \frac{a^s}{S} \log \frac{p(x_{1:n}^s, y_{1:n})}{\frac{a^s}{S}} \\ &\propto \sum_{s=1}^S a^s \log \frac{p(x_{1:n}^s, y_{1:n})}{a^s}. \end{aligned} \quad (10)$$

This equation implies that we can minimize the KL divergence from $q(x_{1:n})$ to $p(x_{1:n}|y_{1:n})$ by finding the \tilde{q}^* that maximizes $\mathcal{L}(x_{1:n})$. Also KL_p relies on Algorithm 2; the only difference is the input of the algorithm, $u^s = p(x_{1:n}^s, y_{1:n}), \forall s$.

4. Total Variation Reshuffling

The TV distance between two particle distributions is defined as

$$\text{TV}(q, p) = \frac{1}{2} \sum_{x \in \mathcal{Q} \cup \mathcal{P}} |q(x) - p(x)| \quad (11)$$

where $\mathcal{Q} = \{x : q(x) > 0\}$ and $\mathcal{P} = \{x : p(x) > 0\}$. The range of TV distance is in $[0, 1]$, zero when the distributions are identical and one when the distributions have disjoint supports.

4.1. Weight Based TV Reshuffling

Recall the multiplicity set \mathcal{A}^S from Equation 5, and let $(\mathcal{X}^n)^S$ be the support of q . We want to find the \tilde{q}^* that

Algorithm 3 Total Variation Reshuffling

Input: $\{u^s\}_{s=1}^S$
Output: $\{i^s\}_{s=1}^S$
 set $a^s = u^s S, \forall s$
 set $\alpha^s = a^s - \lfloor a^s \rfloor, \forall s$
 compute $\alpha = \sum_s \alpha^s$
 order $\alpha^1 \geq \dots \geq \alpha^S$
for $s = 1, \dots, S$ **do**
 if $s \leq \alpha$ **then**
 set $\tilde{g}^s = \lceil a^s \rceil$
 else
 set $\tilde{g}^s = \lfloor a^s \rfloor$
 end if
end for
 map $\{i^s\}_{s=1}^S = h(\{\tilde{g}^s\}_{s=1}^S)$
return $\{i^s\}_{s=1}^S$

minimizes the TV distance

$$\begin{aligned} \text{TV}(q, \tilde{q}) &= \frac{1}{2} \sum_{x_{1:n} \in (\mathcal{X}^n)^S} |q(x_{1:n}) - \tilde{q}(x_{1:n})| \\ &= \frac{1}{2} \sum_s |w^s - \tilde{w}^s| \\ &= \frac{1}{2} \sum_s |w^s - \frac{a^s}{S}|, \end{aligned} \quad (12)$$

which is equivalent to finding $\{a^{*s}\}_{s=1}^S \in \mathcal{A}^S$ that minimizes $\frac{1}{2} \sum_s |w^s S - a^s|$. Let

$$\alpha^s = w^s S - \lfloor w^s S \rfloor, \quad \alpha = \sum_s \alpha^s \quad (13)$$

and note that $\alpha \in \mathbb{Z}_0^+$, since $\sum_s w^s S \in \mathbb{Z}_0^+$ and $\sum_s \lfloor w^s S \rfloor \in \mathbb{Z}_0^+$.

Finally, assume that $\alpha^1 \geq \dots \geq \alpha^S$, and let \tilde{g} be the greedy rounding of w . Computing \tilde{g} according to Algorithm 3, we claim that $\{\tilde{g}^s\}_{s=1}^S = \{a^{*s}\}_{s=1}^S$ and prove it in the Supplementary Materials. When the inputs in Algorithm 3 are the importance weights, $u^s = w^s$ for all s , the resulting reshuffling algorithm is TV_w . Similar to the Algorithm 2, h function maps the ancestor multiplicities to particle indices.

The TV reshuffling can be implemented to run in $O(S \log S)$ time using any sorting algorithm or in time $O(S)$ using radix sort with a negligible loss of numeric precision.

4.2. Likelihood Based TV Reshuffling

TV reshuffling can be applied to $p(x_{1:n}, y_{1:n})$ and, also this, yields an alternative to an ML search heuristic. That

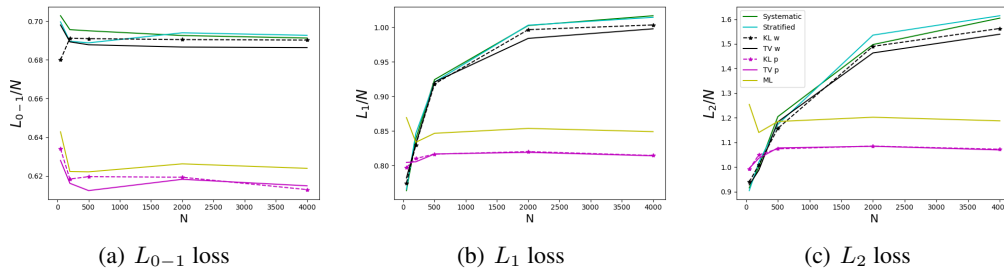


Figure 1: **Bayesian estimators:** Average losses per N on the SV model when $S = 500$. x-axes are the varying number of N whereas the y-axes are the average loss.

is, we can use the TV reshuffling to minimize the TV distance between $q(x_{1:n})$ and $p(x_{1:n}, y_{1:n})$ yielding TV_p – TV reshuffling with likelihoods. Similar to the KL reshuffling, TV_p requires the input of the reshuffling algorithm to be the particle likelihoods, rather than the importance weights.

In Sections 3 and 4, we introduced a class of reshuffling algorithms that perform offspring selection by minimizing separate statistical distances with respect to the importance weights, KL_w and TV_w . Both of the weight based methods are off-the-shelf reshuffling schemes and can be applied to the standard PF algorithm in Algorithm 1 without any workaround.

The likelihood based reshuffling schemes; KL_p and TV_p work with the particle likelihoods, therefore we use them in the updated PF algorithm described in Section 2.2.

5. Experiments

In order to compare the performance of our statistical distance based offspring selection schemes with the stratified and systematic resampling, we use a variety of loss functions (binary loss (L_{0-1}), absolute loss (L_1) and quadratic loss (L_2)) and their corresponding estimators (maximum a posteriori, minimum mean absolute error and minimum mean squared error estimators) (Murphy, 2012). In addition to the mentioned Bayesian estimators, we also use *sampled* estimators where we simply sample a particle trajectory with respect to its importance weight.

We perform two sets of experiments; SMC (using BPF) and pMCMC (using particle Gibbs, PG (Andrieu et al., 2010)). We use two different models and compare the offspring selection schemes in terms of losses, particle degeneracy, parameter estimation, and auto-correlations.

5.1. SMC Experiments

Stochastic volatility (SV) and non-linear (NL) non-Gaussian state space models are used for the SMC experiments. In all the experiments, the number of particles is set to $S = 500$ and the results are averaged over 50 runs unless stated

otherwise.

5.1.1. STOCHASTIC VOLATILITY MODEL

The SV model is popular in real life cases of financial econometrics (Andrieu et al., 2010). Here $Y_{1:N}$ is a sequence of logarithmic returns³ of asset prices $R_{1:N}$, and its volatility is believed to be governed by the latent process $X_{1:N}$. The model is given by

$$\begin{aligned}\mu(x_1) &= \mathcal{N}(0, \sigma^2/(1 - \phi^2)) \\ X_n &= \phi X_{n-1} + \sigma V_n \\ Y_n &= \beta \exp(X_n/2) E_n,\end{aligned}$$

where E_n and V_n are random variables following the standard Gaussian distribution. In our experiments, we assumed the hyper-parameters are given as $(\sigma, \beta, \phi) = (1, 0.5, 0.91)$, the same setup as used in (Doucet & Johansen, 2009).

Figure 1 shows the average losses per time (L/N) of the Bayesian estimators using different offspring selection schemes. The likelihood based methods; ML, KL_p and TV_p , achieve lower loss than the weight based methods; especially when N is large. Also, the weight based methods' L_{0-1} losses are N -invariant, in contrast to its L_1 and L_2 losses. This behaviour can be explained by the Bayesian estimator of the L_{0-1} loss, the maximum a posteriori estimator. The estimator is based on a single trajectory, belonging to the mode of $q(x_{1:N})$.

We show the particle degeneracy of each offspring selection scheme in Figure 2. The plots are generated using a single, $N = 500$ long observation sequence from the set of SV sequences. The ML is not included, since it degenerates as soon as the resampling is done. From the $N = 50$ plots (left column), it can be seen that the likelihood based methods (KL_p and TV_p) degenerate faster, and the final particles share a single common ancestor. The proposed weight based methods (KL_w and TV_w) degenerate less than

³The logarithmic return at time n is given by $y_n = \log(\frac{r_n}{r_{n-1}})$, where r_n is the asset price at time n .

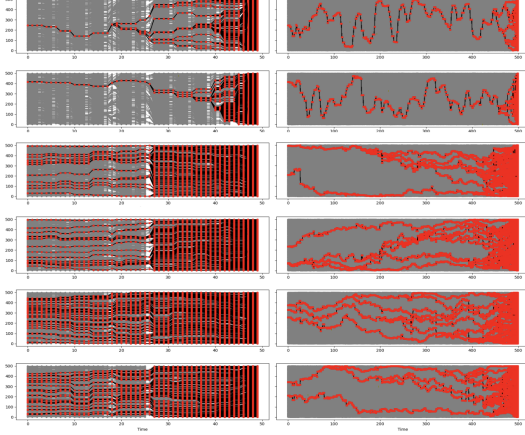


Figure 2: From left to right, the plots depict particle degeneracy when $N \in \{50, 500\}$. The rows correspond to the offspring selection schemes (top to bottom): KL_p , TV_p , KL_w , TV_w , systematic and stratified. x-axes show the time $n \in N$ and y-axes indicate particle indices. The grey lines show how the particles are propagated. The black lines with red dots show the final particles' trajectories.

the likelihood based methods and more than systematic and stratified resampling. The pattern is clearer when $N = 500$. Importantly, all interesting PFs degenerate eventually, regardless of the resampling scheme. As such, and given the results of our likelihood based methods, one should reflect on whether a PF that degenerates necessarily is less useful than one that does not.

In Figure 3, the average L_2 loss per time of the sampled estimators of weight based selection schemes are shown. Here, we focus on weight based approaches, but more results can be found in the Supplementary Materials. Remarkably, as the figure shows, for all $N > 50$ and with $S = 500$, the PF based estimators that build on TV_w and KL_w only need 50 particles in order to obtain a lower L_2 loss than that obtained by those building on stratified or systematic resampling.

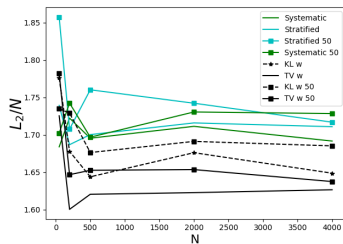


Figure 3: **Sampled estimators:** Average L_2 loss per N for weight based selection schemes in the SV model with different number of particles. The lines with square markers represent $S = 50$ particles, and the rest represents $S = 500$ particles.

5.1.2. NON-LINEAR NON-GAUSSIAN STATE SPACE MODEL

The NL non-Gaussian state space model is an important and often turned to example in the SMC literature (Kitagawa, 1996; Godsill et al., 2004; Andrieu et al., 2010; Smith, 2013). It is an interesting test for PFs, as $p(x_{1:n}|y_{1:n})$ is multimodal (Godsill et al., 2004). In order to excel in this experiment, the PF has to have particles in the vicinity of these modes, i.e. distribute its particles into multiple clusters in the latent space. The model is defined as

$$\begin{aligned} X_1 &\sim \mathcal{N}(0, \sigma_x^2) \\ X_n &= \frac{X_{n-1}}{2} + 25 \frac{X_{n-1}}{1 + X_{n-1}^2} + 8 \cos(1.2n) + V_n \\ Y_n &= \frac{X_n^2}{20} + U_n \end{aligned}$$

where $V_n \sim \mathcal{N}(0, \sigma_x^2)$ and $U_n \sim \mathcal{N}(0, \sigma_y^2)$.

In this group of experiments, we investigate the effects of the parameters $\theta = (\sigma_x^2, \sigma_y^2)$. Observations of varying lengths N are generated with $\theta_1 = (1, 1)$ and $\theta_2 = (10, 10)$. More experiments with different parameters are available in the Supplementary Materials.

As revealed by the experiment illustrated in Figure 4, the ML selection scheme infers states poorly in cases where the true posterior is multimodal. This is natural since ML selects the particle with the highest likelihood, $p(x_{1:n}^s, y_{1:n})$, making the PF distribute all its particles centered at a single mode. Given this severe shortcoming of the ML reshuffling scheme, it will not be considered in the coming experiments. In contrast, both of our likelihood based methods TV_p (in Figure 4(b)) are KL_p (not shown here) able to account for the multimodality.

The performance of Bayesian estimators for different parameter settings are shown in Figure 5. We make the following two observations based on the plots. First, it is important to

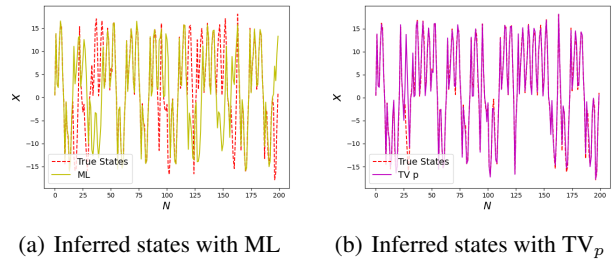
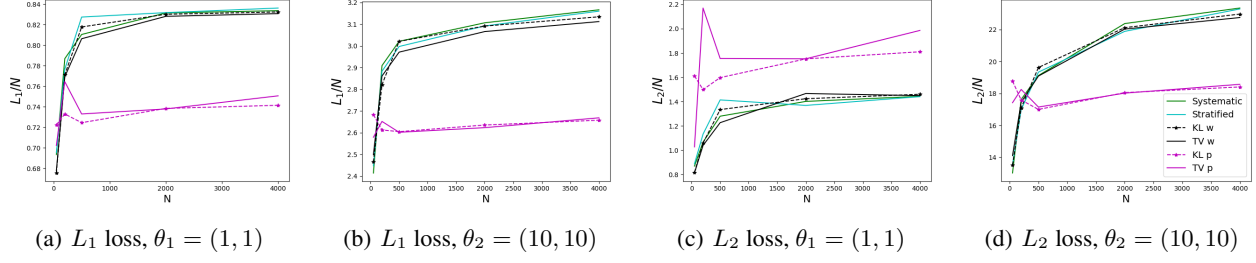


Figure 4: Inferred states in the NL experiment. $\theta = (1, 1)$. The multimodality of the hidden state distribution makes (a) ML unequipped to solve it, in contrast to (b) TV_p . True states are represented by the red dashed line.


 Figure 5: **Bayesian estimators:** Average losses per time for different θ values in the NL experiment.

consider multiple loss functions. L_1 loss plots (Figures 5(a) and 5(b)) indicate the likelihood based schemes provide the best estimates, whereas Figure 5(c) show this is not always the case. Second, our weight based methods obtain smaller losses in three out of the four cases.

5.2. pMCMC Experiments

Here we will present results when, again, considering the SV model, now parameterized by the unknown model parameters $\theta = (\sigma, \beta, \phi)$. Before applying the method to real data, we first consider data generated from the model used in the SMC experiments above, i.e., the true model parameters were $\theta = (\sigma, \beta, \phi) = (1, 0.5, 0.91)$. This allows us to more precisely evaluate the performances of the methods.

The main objective of the following experiments is to evaluate the mixing and parameter estimation capabilities of the PG when using deterministic offspring selection. We use the auto-correlation functions (ACF) to quantify the correlation between samples in the chain as a function of lag. In order to simplify our analysis, we constrain ourselves to comparing with only the stratified resampling scheme.

Inspired by the priors chosen in (Lindsten et al., 2014), we assumed that all parameters were independent, while assigning σ and β inverse Gamma priors (both the shape and rate parameters are set to 0.001). Meanwhile, the posterior over ϕ does not admit a closed-form expression, we modelled ϕ as in (Lindsten et al., 2014) and it was approximated using a rejection sampler (Kim et al., 1998; Lindsten et al., 2014). See Supplementary Materials for details and posterior derivations.

Table 1 shows the parameters estimated by KL_w and stratified resampling with varying time. The estimates are calculated by taking the median over the last 5,000 samples. The closest estimates to the true model parameters are shown in bold. For larger N , KL_w achieves closer parameter estimates. For $N = 500$, we observe that the stratified resampling's β estimate diverges dramatically.

Figure 6 shows the corresponding ACFs. KL_w has strong mixing for small N . Stratified resampling achieves lower auto-correlation values for smaller lags when $N \in \{20, 50\}$; however, it needs larger lag to obtain good mixing when $N \in \{100, 500\}$. One possible explanation why stratified

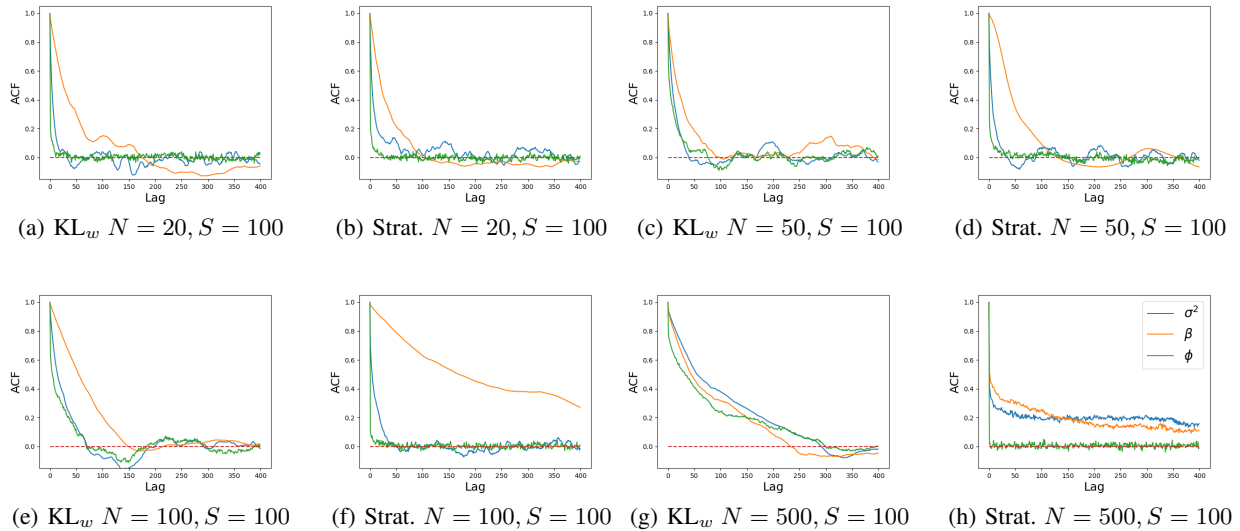

 Figure 6: ACF plots of KL_w and stratified resampling for PG experiments.

Table 1: PG parameter estimation results

N	KL _w			STRATIFIED		
	σ^2	β	ϕ	σ^2	β	ϕ
20	1.42	0.36	0.83	1.37	0.39	0.84
50	0.72	0.49	0.88	1.77	0.14	0.89
100	0.69	0.55	0.94	2.05	0.42	0.86
500	0.56	0.38	0.92	2.11	13.09	0.95
TRUE	1.00	0.50	0.91	1.00	0.50	0.91

immediately gets uncorrelated samples for ϕ when $N = 500$ is due to $g(y_n|x_n)$ in the SV model assigning low probability to all $x_{1:N}$ when β is large (as is the case for stratified, see Table 1). As such the PG is sampling trajectories from a flat distribution, making them varied between iterations. The ϕ parameter’s rejection sampler mainly depends on the sampled trajectory (both in terms of expected value and variance), and so, because of the dissimilarity between them, the sampler draws samples seemingly independent of its previous sample.

Unfortunately, the likelihood based reshuffling schemes converge almost immediately to small variance values, far from the true variances. In short, this occurs since these methods reshuffle, partly, based on the transition probability, which in the SV model obtains extremely high likelihood for the trajectories close to its mean when $\sigma^2 < 1$. In the Supplementary Materials, we further discuss this, and provide plots; however, in the rest of the pMCMC experiments we shall not consider the likelihood based methods.

Finally, we test the performance of our proposed weight based offspring selection methods using Standard and Poor’s (S&P) 500 dataset (Finance, 2021). For the experiments, we extract the data between 2006-04-03 and 2014-03-28, corresponding to $N = 2,011$ as in (Lindsten et al., 2014).

We investigate how the resampling methods work for varying number of particles. Figure 7 shows the ACFs of TV_w and stratified resampling for $N = 2,011$ data, based on the last 5,000 iterations (see the Supplementary Materials for KL_w results). When PG is trained with 20 particles, both TV_w and stratified resampling have low mixing for ϕ . They perform on par for σ^2 and β . Both methods achieve good mixing for ϕ when more particles are used ($S = 100$); however, stratified resampling suffers more for σ^2 and β , even when the lag is large.

6. Conclusion

We introduce two novel offspring selection schemes that are based on minimizing a statistical distance between the normalized particle distribution prior to the offspring selection and the unweighted particle distribution obtained. The first algorithm minimizes the Kullback-Leibler divergence

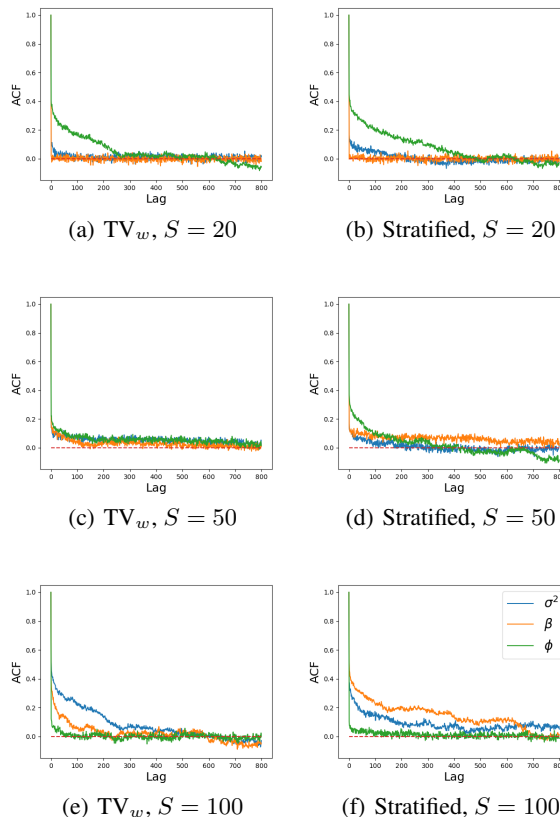


Figure 7: ACF plots of TV_w and stratified resampling for S&P $N = 2,011$ experiments. The columns are TV_w (left) and stratified (right). The rows are the number of particles $S \in \{20, 50, 100\}$, respectively.

and the second algorithm total variation distance. Moreover, both are proved to provide optimal solutions.

We investigated the performance of several offspring selection schemes by embedding them in SMC and pMCMC algorithms for the stochastic volatility model and the non-linear non-Gaussian state space model. Both our novel offspring selection schemes performed better, with respect to the appropriate loss functions, than the state-of-the-art probabilistic resampling schemes, stratified and systematic. Our methods obtain better estimates of parameters and attain less auto-correlation when used in pMCMC. Surprisingly, our offspring selection schemes performed better than stratified and systematic even when we allowed stratified and systematic to use a multiplicative factor of 10 more particles.

As a byproduct, we also obtained two heuristic schemes that instead minimize the statistical distance to the joint distribution. These two had in several cases a desirable performance and we consider them, in particular, to be excellent alternatives for problems that seem fit to a ML based heuristic search.

7. Conclusion

We introduce two novel offspring selection schemes that are based on minimizing a statistical distance between the normalized particle distribution prior to the offspring selection and the unweighted particle distribution obtained. The first algorithm minimizes the Kullback-Leibler divergence and the second algorithm total variation distance. Moreover, both are proved to provide optimal solutions.

We investigated the performance of several offspring selection schemes by embedding them in SMC and pMCMC algorithms for the stochastic volatility model and the nonlinear non-Gaussian state space model. Both our novel offspring selection schemes performed better, with respect to the appropriate loss functions, than the state-of-the-art probabilistic resampling schemes, stratified and systematic. Our methods obtain better estimates of parameters and attain less auto-correlation when used in pMCMC. Surprisingly, our offspring selection schemes performed better than stratified and systematic even when we allowed stratified and systematic to use a multiplicative factor of 10 more particles.

As a byproduct, we also obtained two heuristic schemes that instead minimize the statistical distance to the joint distribution. These two had in several cases a desirable performance and we consider them, in particular, to be excellent alternatives for problems that seem fit to a ML based heuristic search.

Acknowledgements

This project is funded by the Swedish Foundation with Strategic Research grant BD15-0043 and the Swedish Research Council grant 2018-05417-VR. The computations and data handling were enabled by resources provided by the Swedish National Infrastructure for Computing (SNIC), partially funded by the Swedish Research Council through grant agreement no. 2018-05973.

References

- Andrieu, C., Doucet, A., and Holenstein, R. Particle markov chain monte carlo methods. *Journal of the Royal Statistical Society: Series B (Statistical Methodology)*, 72(3): 269–342, 2010.
- Bouchard-Côté, A., Sankararaman, S., and Jordan, M. I. Phylogenetic inference via sequential monte carlo. *Systematic biology*, 61(4):579–593, 2012.
- Douc, R. and Cappé, O. Comparison of resampling schemes for particle filtering. In *ISPA 2005. Proceedings of the 4th International Symposium on Image and Signal Processing and Analysis, 2005.*, pp. 64–69. IEEE, 2005.
- Doucet, A. and Johansen, A. M. A tutorial on particle filtering and smoothing: Fifteen years later. *Handbook of nonlinear filtering*, 12(656-704):3, 2009.
- Doucet, A., De Freitas, N., and Gordon, N. An introduction to sequential monte carlo methods. In *Sequential Monte Carlo methods in practice*, pp. 3–14. Springer, 2001.
- Eade, E. and Drummond, T. Scalable monocular slam. In *2006 IEEE Computer Society Conference on Computer Vision and Pattern Recognition (CVPR'06)*, volume 1, pp. 469–476. IEEE, 2006.
- Finance, Y. S&P 500 (GSPC) historical data, Feb 2021. <https://finance.yahoo.com/quote/^GSPC/history>.
- Fox, D. Kld-sampling: Adaptive particle filters. In *Advances in neural information processing systems*, pp. 713–720, 2002.
- Godsill, S. J., Doucet, A., and West, M. Monte carlo smoothing for nonlinear time series. *Journal of the american statistical association*, 99(465):156–168, 2004.
- Gordon, N. J., Salmond, D. J., and Smith, A. F. Novel approach to nonlinear/non-gaussian bayesian state estimation. In *IEE proceedings F (radar and signal processing)*, volume 140, pp. 107–113. IET, 1993.
- Grisetti, G., Stachniss, C., and Burgard, W. Improving grid-based slam with rao-blackwellized particle filters by adaptive proposals and selective resampling. In *Proceedings of the 2005 IEEE international conference on robotics and automation*, pp. 2432–2437. IEEE, 2005.
- Higuchi, T. Monte carlo filter using the genetic algorithm operators. *Journal of Statistical Computation and Simulation*, 59(1):1–23, 1997.
- Jordan, M. I., Ghahramani, Z., Jaakkola, T. S., and Saul, L. K. An introduction to variational methods for graphical models. *Machine learning*, 37(2):183–233, 1999.
- Kim, S., Shephard, N., and Chib, S. Stochastic volatility: likelihood inference and comparison with arch models. *The review of economic studies*, 65(3):361–393, 1998.
- Kitagawa, G. Monte carlo filter and smoother for non-gaussian nonlinear state space models. *Journal of computational and graphical statistics*, 5(1):1–25, 1996.
- Li, T., Sattar, T. P., and Sun, S. Deterministic resampling: unbiased sampling to avoid sample impoverishment in particle filters. *Signal Processing*, 92(7):1637–1645, 2012.
- Lindsten, F., Jordan, M. I., and Schön, T. B. Particle gibbs with ancestor sampling. *The Journal of Machine Learning Research*, 15(1):2145–2184, 2014.

- Liu, J. S. and Chen, R. Sequential monte carlo methods for dynamic systems. *Journal of the American statistical association*, 93(443):1032–1044, 1998.
- Maddison, C. J., Lawson, J., Tucker, G., Heess, N., Norouzi, M., Mnih, A., Doucet, A., and Teh, Y. Filtering variational objectives. In *Advances in Neural Information Processing Systems*, pp. 6573–6583, 2017.
- Murphy, K. P. *Machine learning: a probabilistic perspective*. MIT press, 2012.
- Naesseth, C. A., Linderman, S. W., Ranganath, R., and Blei, D. M. Variational sequential monte carlo, 2017.
- Pitt, M. K. and Shephard, N. Filtering via simulation: Auxiliary particle filters. *Journal of the American Statistical Association*, 94(446):590–599, 1999. doi: 10.1080/01621459.1999.10474153.
- Saeedi, A., Kulkarni, T. D., Mansinghka, V. K., and Gershman, S. J. Variational particle approximations. *The Journal of Machine Learning Research*, 18(1):2328–2356, 2017.
- Smith, A. *Sequential Monte Carlo methods in practice*. Springer Science & Business Media, 2013.
- Soto, A. Self adaptive particle filter. In *IJCAI*, pp. 1398–1406. Citeseer, 2005.

Statistical Distance Based Deterministic Offspring Selection in SMC Methods Appendix

A. KL Reshuffling Proof

In this section, we show that the KL reshuffling gives the optimal solution, $\tilde{q}^*(x_{1:n}) = \sum_s \frac{a^{*s}}{S} \delta(x_{1:n}^s)$, maximizing the objective function \mathcal{L} (in the weight based approach, \mathcal{L} is the negative KL divergence from $\tilde{q}(x_{1:n})$ to $q(x_{1:n})$, whereas, in the likelihood based approach, \mathcal{L} is the ELBO).

First, the inputs u^s (in the weight based approach, $u^s = w^s$ and in the likelihood based approach, $u^s = p(x_{1:n}^s, y_{1:n})$) are ordered in descending order ($u^1 \geq \dots \geq u^S$). A particle s has multiplicity a^s . We define

$$\begin{aligned} f(a^s, u^s) &= a^s \log \frac{u^s}{a^s} \\ C^+(a^s, u^s) &= f(a^s + 1, u^s) - f(a^s, u^s) \\ C^-(a^s, u^s) &= f(a^s, u^s) - f(a^s - 1, u^s). \end{aligned} \tag{14}$$

where $f(a^s, u^s)$ is the contribution of particle s to \mathcal{L} . C^+ and C^- functions measure how much the \mathcal{L} changes by increasing and decreasing a^s by 1.

\tilde{q}^* is the particle distribution maximizing \mathcal{L} , and let \tilde{q} be the distribution obtained by doing KL reshuffling. We need to prove that $\tilde{q} = \tilde{q}^*$.

Let $g = \operatorname{argmax}_s C^+(a^s, u^s)$ and a^g the current multiplicity of particle g . Consider the first time KL reshuffling obtains an a^g such that $a^g > a^{*g}$. Also, let o be the index of the leftmost particle such that $a^{*o} > a^o$. We will refer this particle as the *optimal* particle, whose optimal multiplicity is a^{*o} . This follows the following statements:

- (i) $a^g = a^{*g} + 1$
- (ii) $-C^+(a^{*g}, u^g) + C^-(a^{*o}, u^o) \geq 0$
- (iii) $C^+(a^g - 1, u^g) - C^+(a^o, u^o) \geq 0$
- (iv) $C^+(a^{*g}, u^g) - C^+(a^o, u^o) \geq 0$

- Item (i) reflects the current situation in the algorithm (recall ‘‘Consider the first time KL reshuffling obtains an a^g such that $a^g > a^{*g}$ ’’).
- Item (ii) states that the cost of changing the optimal solution is greater than or equal to zero.
- Item (iii) shows that it is more or equally beneficial to increase the multiplicity of particle g from $a^g - 1$ to a^g than to increase the multiplicity of particle o from $a^o - 1$ to a^o .
- Item (iv) states the same information as item (iii) since $a^g = a^{*g} + 1$.

By combing the items (ii) and (iv), we get

$$C^-(a^{*o}, u^o) - C^+(a^o, u^o) \geq 0. \tag{15}$$

When we plug in the definitions of C^+ and C^- in Equation 14, we get

$$\begin{aligned} C^-(a^{*o}, u^o) - C^+(a^o, u^o) &= f(a^{*o}, u^o) - f(a^{*o} - 1, u^o) - f(a^o + 1, u^o) + f(a^o, u^o) \\ &= (a^{*o} - (a^{*o} - 1)) \log u^o - (a^o + 1 - a^o) \log u^o \\ &\quad - a^{*o} \log a^{*o} + (a^{*o} - 1) \log(a^{*o} - 1) - a^o \log a^o + (a^o + 1) \log(a^o + 1) \\ &= (a^{*o} - 1) \log(a^{*o} - 1) + (a^o + 1) \log(a^o + 1) - (a^{*o} \log a^{*o} + a^o \log a^o) \end{aligned} \tag{16}$$

Let $Q = a^{*o} + a^o$. Then, the above equation can be written as

$$\begin{aligned} C^-(a^{*o}, u^o) - C^+(a^o, u^o) &= Q \left[\frac{(a^{*o} - 1)}{Q} \log \frac{(a^{*o} - 1)}{Q} + \frac{(a^o + 1)}{Q} \log \frac{(a^o + 1)}{Q} - \left(\frac{a^{*o}}{Q} \log \frac{a^{*o}}{Q} + \frac{a^o}{Q} \log \frac{a^o}{Q} \right) \right] \\ &= Q \left[H \left(\frac{a^{*o}}{Q}, \frac{a^o}{Q} \right) - H \left(\frac{a^{*o} - 1}{Q}, \frac{a^o + 1}{Q} \right) \right], \end{aligned} \tag{17}$$

where $H(\cdot, \cdot)$ is the entropy of a categorical distribution with two categories.

Recall that $a^{*o} > a^o$, and note that there are two cases. First, if $a^{*o} > a^o + 1$, then $H \left(\frac{a^{*o}-1}{Q}, \frac{a^o+1}{Q} \right) > H \left(\frac{a^{*o}}{Q}, \frac{a^o}{Q} \right)$, since the categorical distribution on the left-hand side is flatter than the one on the right-hand side, stating that $C^-(a^{*o}, u^o) - C^+(a^o, u^o) < 0$. This results in a contradiction between Equations (15) and (17), and so this case cannot be true.

The remaining case, $a^{*o} = a^o + 1$, leaves the entropy unchanged ($H \left(\frac{a^{*o}-1}{Q}, \frac{a^o+1}{Q} \right) = H \left(\frac{a^{*o}}{Q}, \frac{a^o}{Q} \right)$), while both Equations (15) and (17) give $C^-(a^{*o}, u^o) = C^+(a^o, u^o)$. Using this equality in any of the items (ii-iv) tells us that incrementing a^g was as beneficial as incrementing a^o according to C^+ , in which case we increase the leftmost particle, either o or g .

Importantly, there may be multiple optimal solutions, but we always choose the solution which is most skewed to the left.

B. TV Reshuffling Proof

Here we prove that $\{\check{g}^s\}_{s=1}^S$ is indeed the optimal set of multiplicities, $\{\check{a}^{*s}\}_{s=1}^S$ minimizing the distance ⁴

$$\begin{aligned} \text{TV}(q, \check{q}) &= \frac{1}{2} \sum_{x_{1:n} \in (\mathcal{X}^n)^S} |q(x_{1:n}) - \check{q}(x_{1:n})| \\ &= \frac{1}{2} \sum_s |w^s - \check{w}^s| \\ &= \frac{1}{2} \sum_s \left| w^s - \frac{\check{g}^s}{S} \right| \end{aligned} \quad (18)$$

Recall from the Section 4.1 that

$$\begin{aligned} \alpha^s &= w^s S - \lfloor w^s S \rfloor \\ &= a^s - \lfloor a^s \rfloor \\ \alpha &= \sum_{s=1}^S \alpha^s \end{aligned} \quad (19)$$

We should note that a^s values do not have to be integers since $a^s = w^s S$.

First, we sort the particles in descending order w.r.t. $\{\alpha^s\}_{s=1}^S$. Once the particles are sorted, α constitutes a decision boundary, deciding which particles should be rewarded with an additional offspring ($\check{g}^s = \lceil a^s \rceil$ if $s \leq \alpha$) and which should not ($\check{g}^s = \lfloor a^s \rfloor$ if $s > \alpha$).

Consider the case where $\check{g} \neq \check{a}^*$, i.e. our solution is not an optimal solution. There may be multiple optimal solutions, so assume that \check{a}^* is the optimal solution which is the most similar (has the lowest TV distance) solution to \check{g} . Further, assume two conditions:

$$\begin{aligned} \text{(i)} \quad & i \text{ is the first index such that } \check{a}^{*i} > \check{g}^i \\ \text{(ii)} \quad & j \text{ is the last index such that } \check{a}^{*j} < \check{g}^j \end{aligned} \quad (20)$$

- Item **(i)** indicates the optimal solution assigned more multiplicity to particle i .
- Item **(ii)** indicates the optimal solution assigned less multiplicity to particle j .

Since \check{a}^* and \check{g} are multiplicities, they are integers, making $|\check{a}^{*i} - \check{g}^i| \geq 1$ and $|\check{a}^{*j} - \check{g}^j| \geq 1$.

There are four cases where particles i and j can be located based on $\{\alpha^s\}_{s=1}^S$ sorting and the arbitrary decision boundary (α). Below, we will cover all these cases and show that \check{g} is an optimal solution by contradiction.

1. $i \leq \alpha$ and $j \leq \alpha$:

Both of the particles are placed at the left-hand side of the decision boundary. The TV reshuffling assigns the rounded up values as the multiplicities; $\check{g}^i = \lceil a^i \rceil$ and $\check{g}^j = \lceil a^j \rceil$. Combining these with the conditions in Equation 20, we get $\check{a}^{*i} > \check{g}^i \geq a^i$ and $\check{a}^{*j} < a^j \leq \check{g}^j$. By changing \check{a}^* (transferring 1 multiplicity from i to j), one obtains a closer solution to \check{g} , which is a better than or as good to the ‘‘optimal’’ solution. Either case, there is a contradiction.

2. $i \leq \alpha$ and $j > \alpha$:

i is placed at the left-hand side and j is placed at the right-hand side of the decision boundary. The TV reshuffling assigns the multiplicities $\check{g}^i = \lceil a^i \rceil$ and $\check{g}^j = \lfloor a^j \rfloor$. Combining these with the conditions in Equation 20, we get $\check{a}^{*i} > \check{g}^i \geq a^i$ and $\check{a}^{*j} < \check{g}^j \leq a^j$. By changing \check{a}^* (transferring 1 multiplicity from i to j), one obtains a closer solution to \check{g} , which is a better than or as good as the ‘‘optimal’’ solution. In either case, there is a contradiction.

⁴This proof is for the weight based TV reshuffling. However, the same proof holds for the likelihood based version as well.

3. $i > \alpha$ and $j \leq \alpha$:

i is placed at the right-hand side and j is placed at the left-hand side of the decision boundary. The TV reshuffling assigns the multiplicities $\check{g}^i = \lfloor a^i \rfloor$ and $\check{g}^j = \lceil a^j \rceil$. Combining these with the conditions in Equation 20, we get $\check{a}^{*i} > a^i \geq \check{g}^i$ and $\check{a}^{*j} < a^j \leq \check{g}^j$. Since a is between \check{a}^* and \check{g} for both of the particles, we should investigate more to see how modifying \check{a}^* changes the solution.

The TV distance between \check{a}^* and a is $(|\check{a}^{*i} - a^i| + |\check{a}^{*j} - a^j|)/2 \geq ((1 - \alpha^i) + \alpha^j)/2$ for particles i and j . The TV distance between \check{g} and a is $(|\check{g}^i - a^i| + |\check{g}^j - a^j|)/2 = (\alpha^i + (1 - \alpha^j))/2$. Since the particles are ordered with respect to their α^s values and i and j are placed to the opposite sides of the decision boundary, we know $\alpha^i \leq \alpha^j$. By using this fact, we see that changing \check{a}^* (transferring 1 multiplicity from i to j), one obtains a closer solution to \check{g} , which is a better than or as good as the “optimal” solution. In either case, there is a contradiction.

4. $i > \alpha$ and $j > \alpha$:

Both of the particles are placed at the right-hand side of the decision boundary. The TV reshuffling assigns the rounded down values as the multiplicities; $\check{g}^i = \lfloor a^i \rfloor$ and $\check{g}^j = \lfloor a^j \rfloor$. Combining these with the conditions in Equation 20, we get $\check{a}^{*i} > a^i \geq \check{g}^i$ and $\check{a}^{*j} < \check{g}^j \leq a^j$. By changing \check{a}^* (transferring 1 multiplicity from i to j), one obtains a closer solution to \check{g} , which is a better than or as good to the “optimal” solution. Either case, there is a contradiction.

Based on the “ \check{a}^* is the optimal solution closest to \check{g} ” assumption and the conditions in Equation 20, we showed that; by modifying \check{a}^* , one can obtain a closer solution to \check{g} , which is a better than or as good to the “optimal” solution. This is a contradiction, therefore \check{g} is an optimal solution.

C. Bootstrap Particle Filter with Likelihood

The likelihood based reshuffling schemes (KL_p and TV_p) require changes in the standard BPF algorithm. The updated algorithm is shown in Algorithm 4.

Algorithm 4 The Bootstrap Particle Filter with Likelihood

Input: $S, \{y_n\}_{n=1}^N$
Output: $q(x_{1:N})$
 initialize $x_1^s \sim \mu(x_1)$
 compute $\tilde{w}_1^s = g(y_1|x_1^s)$
 normalize $w_1^s = \tilde{w}_1^s / (\sum_s \tilde{w}_1^s)$
 compute $p(x_1^s, y_1) = g(y_1|x_1^s)\mu(x_1^s)$
for $n = 2, \dots, N$ **do**
 if $\sum_s (w_{n-1}^s)^{-2} < S/2$ **then**
 select ancestors $\{i_n^s\}_{s=1}^S = \mathcal{R}(\{p(x_{1:n}^s, y_{1:n})\}_{s=1}^S)$
 set $\tilde{w}_{n-1}^s = 1, \forall s$
 else
 set $i_n^s = s, \forall s$
 end if
 propagate $x_n^s \sim f(x_n^s|x_{n-1}^{i_n^s})$
 compute $\tilde{w}_n^s = g(y_n|x_n^s)\tilde{w}_{n-1}^{i_n^s}$
 normalize $w_n^s = \tilde{w}_n^s / (\sum_s \tilde{w}_n^s)$
 compute $p(x_{1:n}^s, y_{1:n}) = g(y_n|x_n^s)f(x_n^s|x_{n-1}^{i_n^s})p(x_{1:n-1}^{i_n^s}, y_{1:n-1})$
end for
return $q(x_{1:N})$

D. Additional Results for SMC SV Experiments

Here, we show the performance of the sampled estimators for L_2 loss. The left subplot of Figure 8 shows the performance comparison when the number of samples are $S = \{20, 500\}$. The right subplot of Figure 8 shows the performance comparison when the number of samples are $S = \{50, 500\}$.

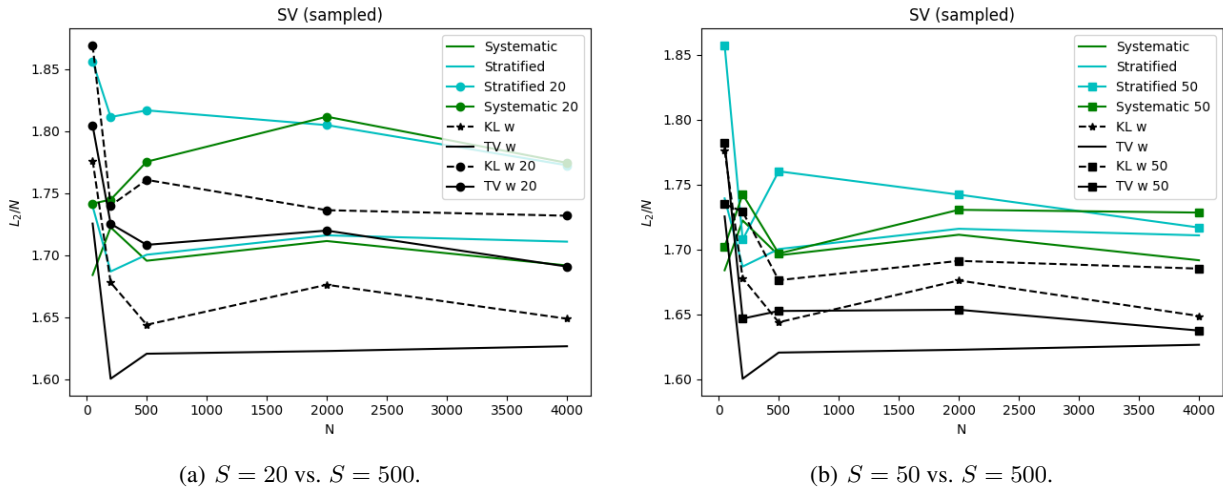


Figure 8: **Sampled estimators:** Average L_2 loss per N for weight based selection schemes. The losses are compared when using 20 (dash-circle) or 50 (dash-square) particles instead of 500.

E. Additional Results for SMC NL Experiments

Here, we present the performance of the Bayesian estimators for L_1 and L_2 losses (Figures 9 and 10, respectively) under different parameter settings.

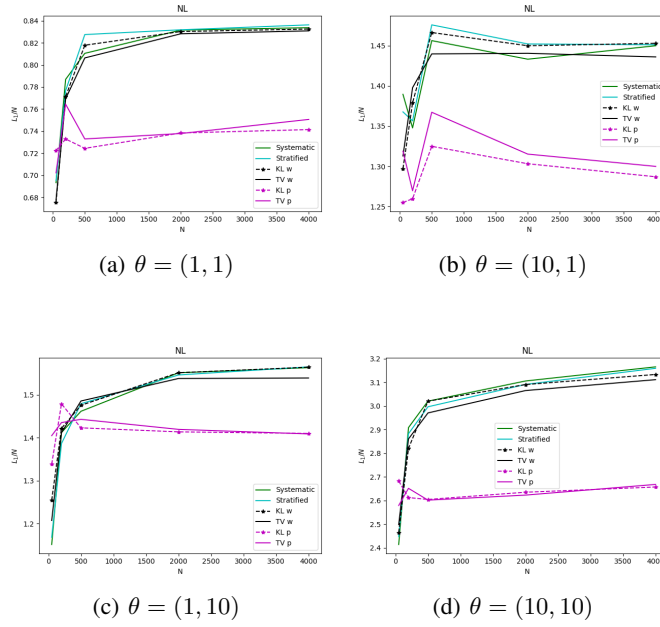


Figure 9: Bayesian estimators: Average L_1 loss.

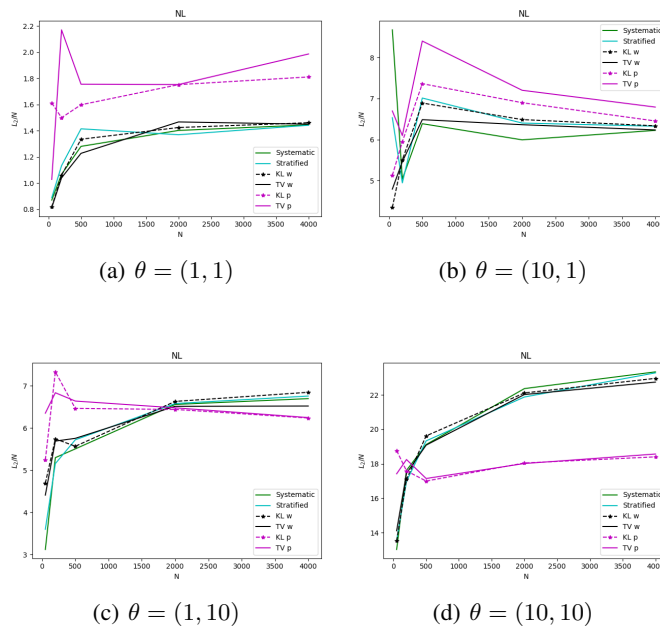


Figure 10: Bayesian estimators: Average L_2 loss.

F. Conjugate Posterior Derivations for PG Experiments

The derivations of the conjugate posteriors for σ^2 and β are very similar, why we only give the derivations for $p(\sigma^2|x_{1:N})$.

First recall that

$$\sigma^2 \sim \mathcal{IG}(\sigma^2|a, b) = \frac{b^a}{\Gamma(a)} (\sigma^2)^{-(a+1)} \exp\left\{\frac{-b}{\sigma^2}\right\}, \quad (21)$$

where Γ is the Gamma function, and that σ^2 is independent of $y_{1:N}$ (as σ^2 is only involved in the transition distribution). This gives us

$$\begin{aligned} p(\sigma^2|x_{1:N}, y_{1:N}) &= p(\sigma^2|x_{1:N}) \propto p(x_{1:N}|\sigma^2)p(\sigma^2) \\ &= \mu(x_1) \prod_{n=2}^N f(x_n|x_{n-1})p(\sigma^2) \end{aligned} \quad (22)$$

Taking the logarithm on both sides of the above equation

$$\begin{aligned} \log p(\sigma^2|x_{1:N}) &= \log \mu(x_1) + \sum_{n=2}^N \log f(x_n|x_{n-1}) + \log p(\sigma^2) \\ &= -\frac{1}{2} \log \frac{2\pi}{1-\phi^2} - \frac{1}{2} \log \sigma^2 - \frac{1}{2} \frac{x_1^2}{1-\phi^2} \\ &\quad - \frac{N-1}{2} \log \sigma^2 - \frac{N-1}{2} \log 2\pi - \frac{1}{2} \sum_{n=2}^N \frac{(x_n - \phi x_{n-1})^2}{\sigma^2} \\ &\quad + a \log b - \log \Gamma(a) - (a+1) \log \sigma^2 - \frac{b}{\sigma^2}, \end{aligned} \quad (23)$$

followed by collecting all terms that are constant in σ^2 into the dummy variable C_{σ^2}

$$\begin{aligned} \log p(\sigma^2|x_{1:N}) &= -\log \sigma^2 \left(\frac{N}{2} + a + 1 \right) \\ &\quad - \frac{1}{\sigma^2} \left[b + \frac{1}{2} x_1^2 (1 - \phi^2) + \frac{1}{2} \sum_{n=2}^N (x_n - \phi x_{n-1})^2 \right] + C_{\sigma^2}, \end{aligned} \quad (24)$$

and, finally, matching this expression to the general form of the \mathcal{IG} distribution (see Equation 21), we arrive at the resulting expression

$$p(\sigma^2|x_{1:N}) = \mathcal{IG} \left(\sigma^2 \left| a + \frac{N}{2}, b + \frac{x_1^2(1-\phi^2)}{2} + \frac{1}{2} \sum_{n=2}^N (x_n - \phi x_{n-1})^2 \right. \right). \quad (25)$$

G. Additional Results for PG Synthetic Data Experiments

Here, we display a serious shortcoming of the likelihood based reshuffling schemes. As can be seen in Figure 11, the PG almost immediately converges to small variance values, far from the true variance, when using KL_p or TV_p .

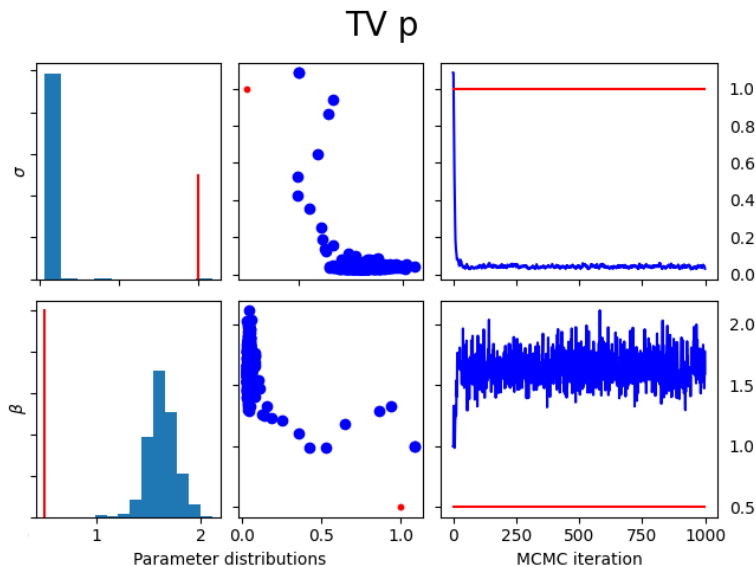


Figure 11: PG approximations of $p(\sigma^2|x_{1:N})$ and $p(\beta|y_{1:N})$ when using TV_p ($N = 100$, $S = 10$, $M = 1000$, no burn-in). Illustrated through histograms, scatter and trace plots. Red markers indicated true parameter values.

In fact, by inspecting the SV model, especially the transition equation, the sensibility of the scheme becomes obvious. KL_p and TV_p both reshuffle based on the transition probability, $p(x_n|x_{n-1}) = \mathcal{N}(x_n|\beta x_{n-1}, \sigma^2)$. Therefore, a smaller transition variance will encourage selection of particles located closest to the transition distribution's mean, in turn forcing the scale parameter in Equation 25 to converge to b . This scale value places the mean and mode of the inverse gamma distribution far below 1 for any reasonable choice of N , which eventually, due to the zero mean in $\mu(x_1)$, causes $x_n \xrightarrow{m} 0 \forall n \in [1, N]$, where m denotes the MCMC iteration. Following this result, we will only focus on the weight based reshuffling schemes in this section (however, we continue discussing KL_p and TV_p in the next chapter). Note, since the PG converged so rapidly to a local mode we only let $M = 1000$ without burn-in.

H. Additional Results for PG Real Data Experiments

We present the ACF results of stratified, TV_w and KL_w (not presented in the main text) in Figure 12.

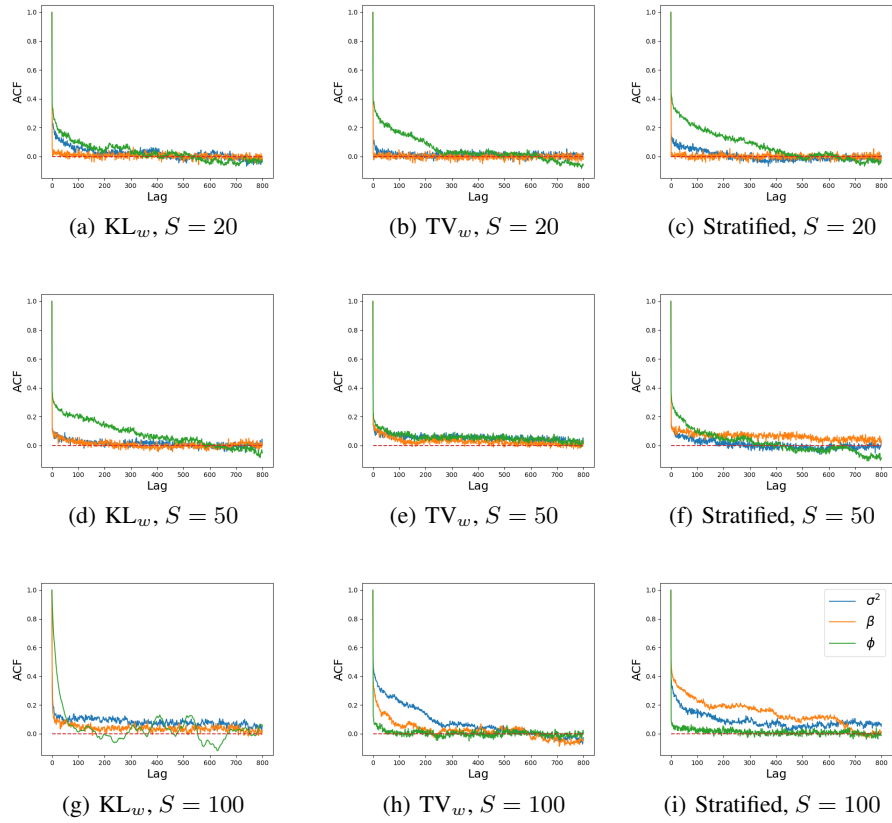


Figure 12: ACF plots of KL_w , TV_w and stratified resampling for S&P $N = 2,011$ experiments. The columns are KL_w (left), TV_w (middle) and stratified (right). The rows are the number of particles $S \in \{20, 50, 100\}$, respectively.

I. Infrastructure Details

All the runs are made on one of the 16 CPUs of an Intel Xeon Gold 6130 processor, which is part of a larger cluster.

J. Particle Gibbs

The particle Gibbs algorithm is shown in Algorithm 5. At each iteration m , the algorithm i) samples the new parameters and ii) samples a trajectory w.r.t. the new parameters and the previous trajectory (see Algorithm 6). The particle index sampled at the end of the kernel, b , is sampled from a Categorical distribution (\mathcal{C}) where the importance weights (or the particle likelihoods, depending on the version of the particle Gibbs) are the category probabilities.

Algorithm 5 Particle Gibbs

Input: $S, \{y_n\}_{n=1}^N$
Output: $\theta^M, x_{1:N}^M$
 initialize $x_{1:N}^1$ and θ^1
for $m = 2, \dots, M$ **do**
 sample parameter $\theta^m \sim p(\theta|y_{1:N}, x_{1:N}^{m-1})$
 sample trajectory $x_{1:N}^m \sim \mathcal{K}(S, y_{1:N}, \theta^m, x_{1:N}^{m-1})$
end for
return $\theta^M, x_{1:N}^M$

Algorithm 6 Particle Gibbs Kernel, \mathcal{K}

Input: $S, \{y_n\}_{n=1}^N, \theta, \mathbf{x}_{1:N}$
Output: $x_{1:N}^b$
 initialize $x_1^s \sim \mu(x_1)$
 set $x_1^S = \mathbf{x}_1$
 compute $w_1^s = 1/S, \forall s$
for $n = 2, \dots, N$ **do**
 if $\sum_s (w_{n-1}^s)^{-2} < S/2$ **then**
 select ancestors $\{i_n^s\}_{s=1}^S = \mathcal{R}(\{w_n^s\}_{s=1}^S)$
 set $i_n^S = S$
 set $\tilde{w}_{n-1}^s = 1, \forall s$
 else
 set $i_n^s = s, \forall s$
 end if
 propagate $x_n^s \sim f(x_n^s|x_{n-1}^{i_n^s}, \theta)$
 set $x_n^S = \mathbf{x}_n$
 compute $\tilde{w}_n^s = g(y_n|x_n^s, \theta)\tilde{w}_{n-1}^s$
 normalize $w_n^s = \tilde{w}_n^s / (\sum_s \tilde{w}_n^s)$
end for
 draw $b = \mathcal{C}(\{w_n^s\}_{s=1}^S)$
return $x_{1:N}^b$

For the likelihood based particle Gibbs, one should make the necessary updates, just like the BPF case.

K. Loss Function and Their Estimators

Table 2 shows the loss functions used in this study and their Bayesian estimators.

Table 2: Loss functions and their estimators

LOSS FUNCTION NAME	LOSS FUNCTION	ESTIMATOR NAME	ESTIMATOR FORMULA
0-1 LOSS	$L_{0-1}(x_n, \hat{x}_n)$	MAXIMUM A POSTERIORI (MAP)	$\hat{x}_n^{\text{MAP}} = \arg \max p(x_n y_{1:N})$
ABSOLUTE LOSS	$L_1(x_n, \hat{x}_n)$	MINIMUM MEAN ABSOLUTE ERROR (MMAE)	$\hat{x}_n^{\text{MMAE}} = \text{med} [p(x_n y_{1:N})]$
QUADRATIC LOSS	$L_2(x_n, \hat{x}_n)$	MINIMUM MEAN SQUARED ERROR (MMSE)	$\hat{x}_n^{\text{MMSE}} = \sum_s w^s x_n^s$

where *med* is the median.

The binary loss is

$$L_{0-1}(x_n, \hat{x}_n) = \begin{cases} 0 & : |x_n - \hat{x}_n| \leq \sigma/2 \\ 1 & : |x_n - \hat{x}_n| > \sigma/2 \end{cases}.$$

The absolute loss is

$$L_1(x_n, \hat{x}_n) = |x_n - \hat{x}_n|.$$

The quadratic loss is

$$L_2(x_n, \hat{x}_n) = (x_n - \hat{x}_n)^2.$$